In presenting the dissertation as a partial fulfillment of the requirements for an advanced degree from the Georgia Institute of Technology, I agree that the Library of the Institution shall make it available for inspection and circulation in accordance with its regulations governing materials of this type. I agree that permission to copy from, or to publish from, this dissertation may be granted by the professor under whose direction it was written, or, in his absence, by the dean of the Graduate Division when such copying or publication is solely for scholarly purposes and does not involve potential financial gain. It is understood that any copying from, or publication of, this dissertation which involves potential financial gain will not be allowed without written permission.

THE VELOCITY DISTRIBUTION IN A LIQUID FILM

A THESIS

Presented to

The Faculty of the Graduate Division

by

Chien-Shiong Lu

In Partial Fulfillment

of the Requirements for the Degree

Master of Science in Mechanical Engineering

Georgia Institute of Technology

September, 1962

4R
12R

THE VELOCITY DISTRIBUTION IN A LIQUID FILM

Approved:

Date Approved by Chairman: 11-5-62

ACKNOWLEDGMENT

Upon completion of this thesis, I make grateful acknowledgments: To Dr. K. G. Picha for his encouragement, helpful advice, and assistance on many matters; to Dr. J. E. Sunderland, my advisor, for his suggestion of the problem and his untiring guidance throughout the pursuit of this investigation; to Dr. C. W. Gorton, for his patient instruction during my entire Master's work; to Dr. H. C. Ward for his assistance in the preparation of my thesis material; to Mr. A. P. Jensen and other staff members of the Rich Electronic Computer Center for their invaluable aid in the numerical calculations; to Miss P. J. Joaquin for patiently typing the manuscript; and to all my friends in the Atlanta area who assisted me in their individual ways.

With thanks to God for His blessings, I dedicate this thesis to my Mother, Mrs. Fong-Shiang Lu, and to Dr. and Mrs. K. H. Chang, in appreciation for their love, care and guidance over the years and their understanding encouragement in connection with my work.

TABLE OF CONTENTS

LIST OF TABLES

LIST OF ILLUSTRATIONS

SUMMARY

This study deals with the determination of the boundary layer thickness and the velocity distribution within a liquid film appearing on a plane surface due to transpiration through a porous wall or the melting of a solid material. The liquid flows over the surface under the influence of gravity. Throughout the study it is assumed that laminar flow and steady state conditions exist and that the pressure distribution in the film and properties of the liquid are constant.

The continuity and momentum equations are set up in integral form. After modifying these equations, a non-linear first-order differential equation for the film thickness is derived. This differential equation is transformed into a non-dimensional form and then integrated numerically by using the Runge-Kutta fourth-order method with the Burroughs 220 Computer. Numerical solutions of the transformed non-linear first-order differential equation are presented in this thesis.

CHAPTER I

INTRODUCTION

In connection with the development of high-speed aircraft, missiles and satellites, a very great effort has been directed in the preceding years toward theoretical and experimental investigations of flow and heat transfer in the laminar boundary layer. As the results of such research, special cooling methods such as ablation cooling, film cooling, transpiration cooling, and mass transfer cooling are frequently used in engineering applications. This study deals with the determination of the boundary layer thickness and the velocity distribution within a liquid film appearing on a plane surface due to transpiration through a porous wall or the melting of a solid material. In using transpiration effects to cool a body, a fluid (liquid or gas) is caused to flow through a porous medium. The fluid reduces the rate of heat transfer to the body, because it absorbs some energy due to its own thermal capacitance and, as it leaves the body, it reduces the convective heat transfer coefficient between the environment and the surface of the porous medium. If the fluid is a liquid, heat must be transferred through a layer of liquid which is flowing from the surface. For ablation cooling, if a body is permitted to melt, then the melted liquid layer will provide a "thermal barrier" which will reduce the rate of heat transfer between the environment and the (solid) surface of the body. In order to show the present status of these problems, a brief review of the literature related to them will be given.

1-1. Ablation Problem

It is well known that solid bodies falling into the atmosphere of the earth from outer space attain very high speeds. Thus the skin of these bodies is subject to excessive heating by internal friction within the boundary layer which surrounds the bodies. This phenomenon is usually called aerodynamic heating. A powerful means of protecting a surface against the thermal influence during high-speed boundary-layer flow is called ablation cooling. The skin is manufactured of such a material that it melts, decomposes, or sublimes when the temperature is increased by aerodynamic heating. An understanding of flow during melting is fundamental to an overall understanding of the ablation problem.

An excellent summary of the status of the ablation problem has been given by Adams (1)[1]. He also presented data comparing the effectiveness of glassy materials in providing protection and insulation for a recoverable satellite exposed to a rather moderate heat load during re-entry. An approximate analytical investigation of glassy substances in general was made by Bethe and Adams (2). This analysis accounts for the large viscosity variation through the liquid layer and treats stagnation ablation with and without evaporation. Roberts (3) studied the effect of the viscous melt, continuously removed, on the melting rate of a solid. Lees (4) obtained approximate analytical solutions for melting ablation under the assumption of constant viscosity through the liquid layer. Sutton (5) treated ablation at the stagnation point and obtained numerical solutions for a certain

---

[1]Numbers in parentheses refer to citations in the Bibliography, except where they are equation numbers.

glassy material subjected to hypersonic flight conditions. He pointed out the important influence of viscosity on the surface temperature. In order to understand the many mechanisms involved in ablation, Turcotte (6) investigated theoretically and experimentally the incompressible stagnation point melting of ice from a hemisphere in a hot humid stream of air. Citron (7) presented solutions for the steady state temperature distribution, the steady state melting rate and the amount of material melted and ablated from a semi-infinite medium subjected to a heat flux at the melting face.

1-2. Transpiration Cooling

A very effective means for protecting a surface exposed to hot gas streams is transpiration cooling. Such a cooling process can be realized by the use of a porous surface through which a coolant gas is forced or injected in a direction opposite to that of the heat flow. On the surface of the porous wall the cooling fluid builds a film that absorbs a considerable quantity of heat and keeps the wall cool. Mass transfer cooling is the same as transpiration cooling, except the properties of the coolant are different from those of the outer streams.

In 1944, Duwez and his associates (8) investigated porous wall cooling experimentally. They found that either a liquid or gas may be used as a good coolant. They also pointed out that when the velocity and the temperature of outer streams are constant, the surface temperature of the porous wall decreases as the flow rate of coolant increases. Wheeler and Duwez (9) theoretically and experimentally studied heat transfer and pressure drop in transpiration-cooled porous tubes for hydrogen and nitrogen. Berman (10) investigated the effect of low Reynolds numbers suction on the two-dimensional steady-state incompressible laminar flow of a fluid in channels with porous walls. Yuan (11) extended Berman's investigation to higher Reynolds numbers. Eckert and Livingood (12) show that transpiration cooling is superior to other known aircooling methods. This cooling method requires the use of much less cooling air than the convection cooling requires. The boundary problem for the case of two-dimensional steady-state incompressible flow of a fluid in a porous tube with uniform injection was considered by Yuan and Finkelstein (13). Hartnett and Eckert (14) were concerned with the prediction of the rate of heat transfer, skin friction, and required coolant flows for transpiration-cooled surfaces. Analytical predictions were given by Eckert, Schneider, Hayday, and Larson (15) for the development of the velocity, temperature, and concentration fields in a laminar air boundary layer on a transpiration-cooled flat porous plate. Leadon (16) investigated the influence of mass transfer on the transition from laminar to turbulent flow. Fundamental concepts of transpiration cooling were discussed by Eckert and Drake (17). Beusman and Weisman (18) examined recent pertinent data and extended their studies to the molecular weights and heats of vaporization of more promising transpiration coolants, such as water and lithium. The effect of mass transfer on free convection was studied by Eichhorn (19). Mouradian (20) determined the velocity and temperature distributions in a liquid film by developing a new type of analysis which is based on the method of isoclines.

1-3. Specific Objectives

The purpose of this study is to investigate the laminar hydrodynamic boundary layer thickness and the velocity distribution within a liquid film appearing on a plane surface due to transpiration through a porous wall or the melting of a solid material. Throughout the study it is assumed that laminar flow and steady state conditions exist and that the pressure distribution in the film and properties of the liquid are constant. The flow is regarded as two-dimensional. Fluid is directed through the surface in the y-direction (as shown in Fig. 1) or appears on the solid-liquid interface as in the case of a melting solid. Then, the fluid flows along the surface of the wall, represented by the x-axis, under the influence of gravity and a liquid boundary layer is created.

The continuity and momentum equations are set up in integral form. After modifying these equations and making use of a process of substitution and integration, a non-linear first-order differential equation for the film thickness is derived. This differential equation is transformed into a non-dimensional form. The Runge-Kutta fourth-order method of Merson (21) is used with the Burroughs 220 Computer in solving the non-dimensional differential equation for the hydrodynamic boundary layer thickness.

This study can be considered as an extension and verification of one part of Mouradian's work. The main differences between this study and the work of Mouradian are the form of the non-linear first-order differential equation for the hydrodynamic boundary layer thickness and the use of a different method to obtain the solutions.

CHAPTER II

THE MATHEMATICAL DEVELOPMENT OF THE LAMINAR HYDRODYNAMIC BOUNDARY LAYER

2-1. The Development of Continuity and Momentum Equations

In most cases, the mathematical difficulties associated with exact solutions of laminar boundary layer problems are considerable. Therefore, it is important to devise an approximate method, which satisfies the differential equations of boundary layer flow only in an average boundary layer thickness and does not try to satisfy the velocity distribution for every individual fluid particle. For this purpose, a control volume abcd, with a unit length in the z-direction, as shown in Figure 1, is chosen. The present analysis will be based on the following postulates:

(a) The flow is two-dimensional.

(b) The flow occurs under the influence of gravity.

(c) The flow is laminar and steady with respect to time.

(d) The fluid is incompressible.

(e) The pressure distribution in the film is constant.

(f) The physical properties of the liquid are constant.

(g) The "feed-in" velocity, V_o, is constant.

For a unit length in the z-direction, the mass-flow rates across the individual faces of the control volume are listed below:

Boundary	Mass-flow Rate
ab	$\rho\int_0^\delta u\,dy$

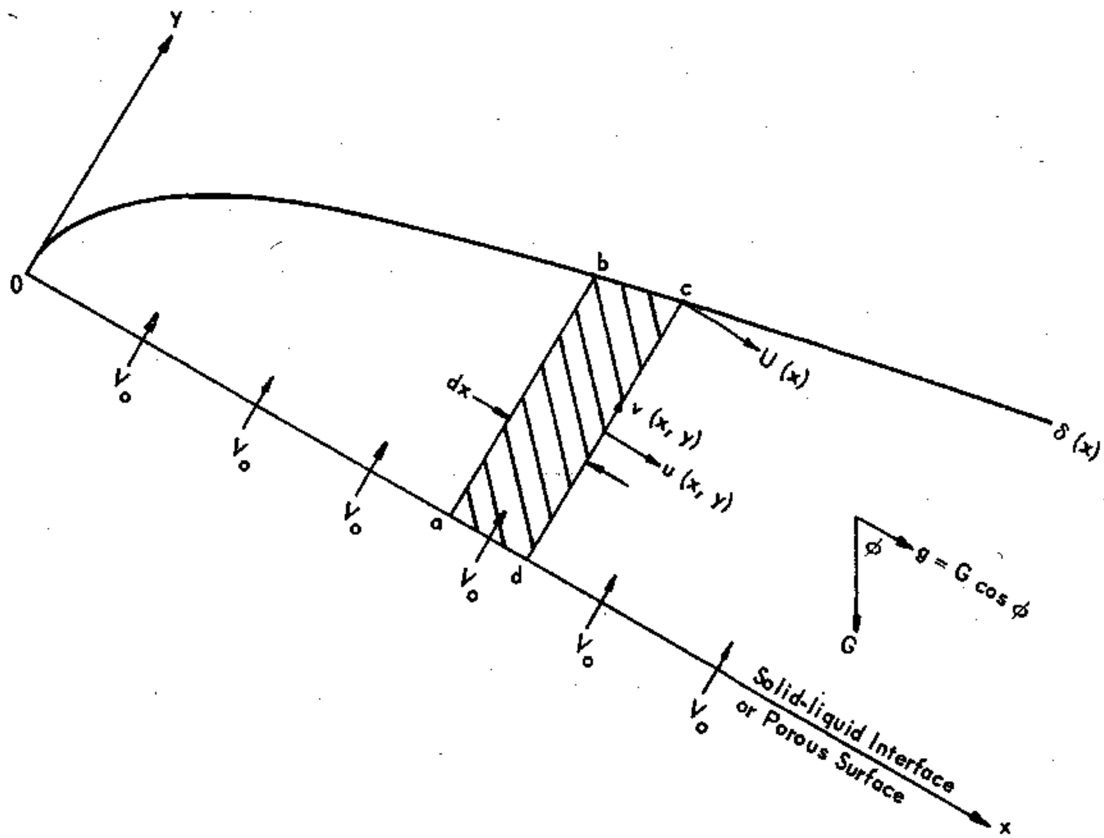

Figure 1. Control Volume for Continuity and Momentum Analysis of a Boundary Layer.

Boundary	Mass-flow Rate
bc	0
cd	$\rho \int_0^\delta udy + \rho \left[\frac{\partial}{\partial x} \int_0^\delta udy\right] dx$
da	$\rho \; V_o \, dx$

For steady state condition, the continuity equation equates the rate of mass influx to the rate of mass efflux. Then

$$\rho \int_0^\delta udy + \rho \; V_o \, dx = \rho \int_0^\delta udy + \rho \left[\frac{\partial}{\partial x} \int_0^\delta udy\right] dx$$

From this relationship, the equation of continuity is obtained, as follows:

$$\frac{\partial}{\partial x} \int_0^\delta udy = V_o \tag{2-1}$$

The rates of x-momentum across the individual faces of the control volume are listed below:

Boundary	The x-Momentum per Unit Time
ab	$\rho \int_0^\delta u^2 \, dy$
bc	0
cd	$\rho \int_0^\delta u^2 \, dy + \rho \left[\frac{\partial}{\partial x} \int_0^\delta u^2 \, dy\right] dx$
da	0

Subtracting the rate of x-momentum inflow from the rate of x-momentum outflow, the increase of x-momentum per unit time of the fluid in the control volume is expressed

$$\frac{\Sigma M_x}{\Delta T} = \rho \left[\frac{\partial}{\partial x} \int_0^\delta u^2 \, dy \right] dx$$

The external forces acting on the control volume in the x-direction are:

Gravitational force $\rho \; g \; \delta \; dx$

and

Shear force along the solid-liquid interface or the porous surface $-\tau_w \, dx = - \rho \, \nu \left(\frac{\partial u}{\partial y}\right)_{y=0} dx$

Then the summation of these external forces is

$$\Sigma F_x = \rho \; g \; \delta \; dx - \rho \; \nu \left(\frac{\partial u}{\partial y}\right)_{y=0} dx$$

From Newton's second law

$$\Sigma F_x = \frac{\Sigma M_x}{\Delta T}$$

Hence

$$\rho \left| \frac{\partial}{\partial x} \int_0^\delta u^2 \, dy \right| dx = \rho g \, \delta \, dx - \rho \nu \left(\frac{\partial u}{\partial y}\right)_{y=0} dx$$

or

$$\frac{\partial}{\partial x} \int_0^\delta u^2 \, dy = g\delta - \nu \left(\frac{\partial u}{\partial y}\right)_{y=0} \qquad (2\text{-}2)$$

This is the momentum equation.

2-2. Boundary Conditions

When writing an expression for the velocity profile, it is necessary to satisfy certain boundary conditions which the actual velocity profile is known to fulfill or to approximate. Such conditions can be found at $y=0$ or at $y=\delta$. It is known that

$$u = 0 \quad \text{at} \quad y = 0 \qquad (2\text{-}3a)$$

$$u = U \quad \text{at} \quad y = \delta \qquad (2\text{-}3b)$$

$$\left(\frac{\partial u}{\partial y}\right)_{y=\delta} = 0 \quad \text{at} \quad y = \delta \qquad (2\text{-}3c)$$

$$V_o \left(\frac{\partial u}{\partial y}\right)_{y=0} = g + \nu\left(\frac{\partial^2 u}{\partial y^2}\right)_{y=0} \quad \text{at } y = 0 \qquad (2\text{-}3d)$$

Equation (2-3a) comes from a no-slip assumption at the liquid-solid surface or the porous surface. Equations (2-3b) and (2-3c) are based on the assumption that at the outer edge of the boundary layer the parallel component u becomes equal to that in the outer flow and here no shear stress exists. Equation (2-3d) results from applying the Navier-Stokes momentum equation in the x-direction at the plane $y = 0$.

2-3. Velocity Distribution

As shown in Appendix III, Mouradian (20) used the four boundary conditions to get a polynominal of the fourth degree for the velocity function in terms of the dimensionless distance from the wall. His results are

$$\frac{u(x,y)}{U(x)} = b\ (\eta - 2\,\eta^2 + \eta^3) + (3\,\eta^2 - 2\,\eta^3)$$

where

$$b = \frac{\frac{g\delta^2}{\nu U} + 6}{\frac{V_o\delta}{\nu} + 4}$$

It can be seen that the velocity distribution U as given in the above equations depends on η, b, and δ. Mouradian combined these equations but the final form obtained is sufficiently complex that a numerical solution would be very difficult to obtain. He also showed that the final solution is not very different from the solution of a differential equation which can be derived by an assumption that the velocity function is a polynomial of the third degree. With the first three boundary conditions, Equations (2-3a) to (2-3c), a polynomial of the third degree for the velocity function is assumed as follows:

$$\frac{u(x,y)}{U(x)} = f(\eta) = A + B\eta + C\eta^2 \qquad (2\text{-}4)$$

where A, B, and C are assumed to be constants and $f(\eta)$ is a function of η only. This means that the velocity profiles are similar at every x position. These coefficients are determined by applying the first three boundary conditions.

Equation (2-3a) gives:

$$A = 0 \qquad (2\text{-}5a)$$

From Equation (2-3b), that is at $\eta=1$, $f(\eta)=1$,

$$B + C = 1 \qquad (2\text{-}5b)$$

The first derivative of Equation (2-4) with respect to y, is:

$$\frac{\partial u}{\partial y} = U\left[\frac{B}{\delta} + \frac{2C}{\delta}\left(\frac{y}{\delta}\right)\right]$$

At $y = \delta$

$$\left(\frac{\partial u}{\partial y}\right)_{y=\delta} = \frac{U}{\delta}(B + 2C)$$

Then, Equation (2-3c) gives:

$$B + 2C = 0 \qquad (2\text{-}5c)$$

From Equations (2-5b) and (2-5c)

$$B = 2 \qquad (2\text{-}5d)$$

Substituting Equation (2-5d) into Equation (2-5b) gives:

$$C = -1 \qquad (2\text{-}5e)$$

Substituting Equations (2-5a), (2-5d), and (2-5e) into Equation (2-4) gives:

$$\frac{u}{U} = f(\eta) = 2\eta - \eta^2 \qquad (2\text{-}6)$$

In Appendix II, it is shown that Equation (2-6) can be expressed in the following non-dimensional form:

$$\frac{u^*}{U^*} = 2\eta - \eta^2 \qquad (2\text{-}7)$$

2-4. Rewriting Continuity and Momentum Equations

It is found that the following terms appear in Equation (2-1) and

(2-2):

$$\int_{o}^{\delta} u dy \;; \quad \left(\frac{\partial u}{\partial y}\right)_{y=o} \;; \quad \int_{o}^{\delta} u^2 dy$$

In this section, it will be shown how these terms can be rewritten in simple form.

If the velocity profiles are assumed similar, the velocity distribution equation has the form:

$$\frac{u}{U} = f\left(\frac{y}{\delta(x)}\right) = f(\eta) \qquad (2\text{-}8)$$

where

$$\eta = \frac{y}{\delta}$$

If $y = 0$, then $\eta = 0$. Similarly, if $y = \delta$, $\eta = 1$. The relationship between dy and $d\eta$ is: $dy = \delta \cdot d\eta$. The integral in the continuity equation, Equation (2-1), can now be rewritten, as follows:

$$\int_{o}^{\delta} u dy = \int_{o}^{\delta} U\ f(\eta)\ dy = U\delta \int_{\eta=o}^{1} f(\eta)\ d\eta = U\delta\alpha_1 \qquad (2\text{-}9a)$$

where

$$\alpha_1 = \int_{o}^{1} f(\eta)\ d\eta$$

The integral in the momentum equation, Equation (2-2), can be rewritten

$$\int_{o}^{\delta} u^2 dy = \int_{o}^{\delta} U^2 f^2(\eta)\ dy = U^2\ \delta \int_{o}^{1} f^2(\eta)\ d\eta = U^2\delta\alpha_2 \qquad (2\text{-}9b)$$

Where

$$\alpha_2 = \int_{o}^{1} f^2(\eta)\ d\eta$$

Taking the first derivative of Equation (2-8) with respect to y gives:

$$\frac{\partial u}{\partial y} = \frac{\partial\left[Uf(\eta)\right]}{\partial y} = \frac{U}{\delta}\,\frac{df(\eta)}{d\eta} = \frac{U}{\delta}\,f'(\eta)$$

Then, the partial differential term on the right-hand side of Equation (2-2) can be rewritten, as follows:

$$\left(\frac{\partial u}{\partial y}\right)_{y=o} = \frac{U}{\delta}\,f'(0) = \frac{U}{\delta}\beta_1 \tag{2-9c}$$

where

$$\beta_1 = f'(0)$$

Considering the case of

$$f(\eta) = 2\eta - \eta^2 \tag{2-6}$$

$$\alpha_1 = \int_o^1 (2\eta - \eta^2)\, d\eta = \left[\frac{2\eta^2}{2} - \frac{\eta^3}{3}\right]_o^1 = 1 - \frac{1}{3} = \frac{2}{3}$$

$$\alpha_2 = \int_o^1 (2\eta - \eta^2)\, d\eta = (4\eta^2 - 4\eta^3 + \eta^4)\, d\eta$$

$$= \left[\frac{4\eta^3}{3} - \eta^4 + \frac{\eta^5}{5}\right]_o^1 = \left[\frac{4}{3} - 1 + \frac{1}{5}\right] = \frac{8}{15}$$

Differentiating Equation (2-6) with respect to η gives:

$$f'(\eta) = \frac{f(\eta)}{\partial\eta} = 2 - 2\eta$$

Then

$$\beta_1 = f'(0) = 2$$

Substituting the values of α_1, α_2, and β_1 into Equations (2-9a), (2-9b), and (2-9c), respectively, gives:

$$\int_o^{\delta} u dy = \frac{2}{3} U\delta \tag{2-9d}$$

$$\int_o^{\delta} u^2 dy = \frac{8}{15} U^2\delta \tag{2-9e}$$

$$\left(\frac{\partial u}{\partial y}\right)_{y=o} = 2\,\frac{U}{\delta} \tag{2-9f}$$

Substituting Equation (2-9d) into Equation (2-1) yields:

$$\frac{\partial}{\partial x} \int_o^{\delta} u dy = \frac{2}{3} \frac{\partial}{\partial x} (U\delta) = V_o$$

Because, at x=0, δ=0 and U never approaches α; therefore, Uδ=0, at x=0. Now, integrating the above partial differential equation with respect to x becomes:

$$\frac{2}{3} \int_o^{U\delta} d\,(U\delta) = \int_o^{x} V_o\, dx$$

Then, the continuity equation becomes:

$$U = \frac{3}{2} \frac{V_o x}{\delta} \tag{2-10}$$

or, in dimensionless form:

$$U^* = \frac{3}{2} \frac{x^*}{\delta^*} \tag{2-11}$$

Substituting Equations (2-9e) and (2-9f) into Equation (2-2), the momentum equation becomes:

$$\frac{8}{15}\frac{\partial}{\partial x}(U^2\delta) = g\delta - 2\nu\frac{U}{\delta} \tag{2-12}$$

Substituting Equation (2-10) into (2-12) yields:

$$\frac{6}{5}V_o^{\,2}\frac{d}{dx}\left(\frac{x^2}{\delta}\right) = g\,\delta - 3\nu V_o\frac{x}{\delta^2}$$

or

$$\frac{d}{dx}\left(\frac{x^2}{\delta}\right) = \frac{5}{6}\frac{g}{V_o}\delta - \frac{5}{2}\frac{\nu}{V_o}\frac{x}{\delta^2}$$

or

$$\frac{x^2}{\delta^2}\frac{d\delta}{dx} = \frac{5}{2}\frac{\nu}{V_o}\frac{x}{\delta^2} + 2\frac{x}{\delta^2} - \frac{5}{6}\frac{g}{V_o^{\,2}}\delta.$$

Rearranging, the differential equation for the film thickness becomes

$$\frac{d\delta}{dx} = \frac{5}{2}\frac{\nu}{V_o}\frac{1}{x} + 2\frac{\delta}{x} - \frac{5}{6}\frac{g}{V_o^{\,2}}\frac{\delta^3}{x^2} \tag{2-13}$$

By a similar analysis, Mouradian (20) assumed that

$$\frac{u}{U} = 2\eta - \eta^2$$

and derived Equation (2-13). From Appendix II, Equation (2-13) in non-dimensional form is expressed, as follows:

$$\frac{d\delta^*}{dx^*} = \frac{5}{2}\frac{1}{x^*} + 2\frac{\delta^*}{x^*} - \frac{5}{6}Q^*\frac{\delta^{*3}}{x^{*2}} \tag{2-14a}$$

or

$$\frac{d\delta^*}{dx^*} = \left(\frac{5}{2} + 2\delta^* - \frac{5}{6} Q^* \frac{\delta^{*3}}{x^*} \right) \frac{1}{x^*} \qquad (2\text{-}14b)$$

This non-linear first-order differential equation for the film thickness will be solved by the Runge-Kutta fourth-order method with the Burroughs 220 Computer.

CHAPTER III

THE METHOD OF SOLUTION

In order to determine the film thickness, Equation (2-14b) must be integrated. Due to the non-linear nature of this equation, a mathematical solution of this equation has not been found. As a result, it will be integrated by a numerical method.

In dealing with this equation, many numerical methods may be used. The Adams-Bashforth method, which replaces the derivative of a function by a polynomial and integrates that polynomial over an interval, gives reliable accuracy. This method assumes that an initial table of values has been computed by means of a Taylor's series or other methods. The Milne method is quite accurate but it is unfavorable from the point of view of stability (22) (23). This method is not self-starting, since it needs four given values for starting the calculation procedure. The use of Taylor's series has the difficulty in finding successive derivatives of the given differential equation. A considerable amount of programming is required for the given equation if this method is used with an electronic computer. For application to high-speed digital computers, the Runge-Kutta method appears very useful for the solution of the given equation if the step-size is small enough.

It is known that the most noted one of the Runge-Kutta fourth-order sets of formula is:

$$y_{n+1} = y_n + \frac{1}{6} (k_1 + 2k_2 + 2k_3 + k_4) + 0 \ (h^5)$$

where

$$k_1 = hf\ (x, y)$$

$$k_2 = hf\ (x + \frac{h}{2},\ y + \frac{k_1}{2})$$

$$k_3 = hf\ (x + \frac{h}{2},\ y + \frac{k_2}{2})$$

$$k_4 = hf\ (x + h,\ y + k_3)$$

This Runge-Kutta method retains the Taylor's series expansion up the term of y^{iv} in each step and is extremely easy to program (24). The stability of this method is good (25). When calculating y_{n+1} the only information required is x_n, y_n, the step-size h and the form of the differential equation as defined by f(x,y). This method also has the advantage of simplicity in the coefficients of k_n (n=1, 2, 3...). Usually the simplicity of the coefficients enables a short program to be written. However, this method does not contain in itself any simple means for estimating the error. Lance (21) introduces the Runge-Kutta method of Merson (this method is a slight modification of the Runge-Kutta technique). The formula is:

$$y_{n+1} = y_n + \frac{1}{2}\ (k_1 + 4k_4 + k_5) + 0\ (h^5)$$

where

$$k_1 = \frac{1}{3}\ hf\ (x_n, y_n)$$

$$k_2 = \frac{1}{3}\ hf\ (x_n + \frac{1}{3} h,\ y_n + k_1)$$

$$k_3 = \frac{1}{3} hf\ (x_n + \frac{1}{3} h,\ y_n + \frac{1}{2} k_1 + \frac{1}{2} k_2)$$

$$k_4 = \frac{1}{3} hf\ (x_n + \frac{1}{2} h,\ y_n + \frac{3}{8} k_1 + \frac{9}{8} k_3)$$

$$k_5 = \frac{1}{3} hf\ (x_n + h,\ y_n + \frac{3}{2} k_1 - \frac{9}{2} k_3 + 6k_4).$$

The unique advantage of the above method is that an estimate of the truncation error, ϵ, which is defined here as the error in y in making the step from x_n to x_{n+1}, is given by

$$\epsilon = 0.2k_1 - 0.9k_3 + 0.8k_4 - 0.1k_5$$

Although this method requires five substitutions into the given differential equation, this is not a drawback according to the differential Equation (2-14b) with regard to the register storage capacity of the Burroughs 220. Therefore, Merson's modification of the Runge-Kutta fourth-order method is used to solve Equation (2-14b) with the Burroughs 220 Computer. The results of this work may be found in Appendix VII.

CHAPTER IV

DISCUSSION OF RESULTS

The calculations of this work are carried out by Merson's modification of the Runge-Kutta fourth-order ~~method~~ (21) with the Burroughs 220 Computer. The computer is operated in conformity with a program which is based on Equation (2-14b) and on the assumed starting point ($x^* = 0.0702$, $\delta^*=0$, as discussed in Appendix V) as well as on the different values of the non-dimensional parameter Q^*. The results of the calculation are obtained in the form of a typewritten numerical table which directly gives X (standing for x^*), Y (representing δ^*), K1, K2, K3, K4, and K5, as shown in Table 2.

As mentioned in Chapter III, Merson's method presented a formula for estimating the truncation error, as follows:

$$\varepsilon = 0.2k_1 - 0.9k_3 + 0.8k_4 - 0.1k_5.$$

By substituting the values of K_1, K_3, K_4 and K_5 in Table 2 into this equation, errors at the corresponding points of x^* can be calculated. It is found that for the same step-size as x^* increases, the absolute value of ε decreases. For example, $x^* = 0.0702$, $\varepsilon = +0.0000103$; $x^* = 0.1002$, $\varepsilon = +0.0000056$; $x^* = 0.1502$, $\varepsilon = +0.0000019$; $x^* = 0.20002$, $\varepsilon = -0.0000006$; $x^* = 0.2502$, $\varepsilon = -0.0000005$.

In order to confirm that the solution of the present work is reasonable and approaches closely to the desired solution of Equation

(2-14b), Mouradian's solution (20) is transformed into a non-dimensional form

$$x^* = \frac{\frac{1}{3} Q^* \ \delta^{*3}}{\frac{2}{5} \phi_G^* \ \delta^* + 1} \tag{4-1}$$

Mouradian pointed out that the desired solution curve slowly varies from $\phi_G^* = \frac{5}{3}$ to $\phi_{G^*} = \frac{3}{2}$. Therefore, if these two values are substituted into the above equation separately, expressions for the upper and lower limits of the desired solution can be obtained, as follows:

$$x^* = \frac{Q^* \ \delta^*}{2\delta^* + 3} \tag{4-2}$$

and

$$x^* = \frac{Q^* \ \delta^*}{1.8 \ \delta^* + 3} \tag{4-3}$$

As shown in Figs. 2, 3, and 4, comparisons are made between the numerical solution and the curves of the upper and lower limits of the desired solution. Since the curves of the present study are bounded by the curves of the upper and lower limits, the numerical solution of Equation (2-14b) is quite satisfactory, even though the starting point is assumed to be the point $x^* = 0.0702$, $\delta^* = 0$ instead of $x^* = 0$, $\delta^* = 0$. These comparisons also tell that the numerical solution of the present study is quite close to the lower limit curve. Therefore, Equation (4-3), which expressed the lower limit of the desired solution, may be used as the approximate solution of Equation (2-14b) without serious error.

The cases for $Q^* = 10^{-3}$, 10^{-2}, 0.1, 1.0, 10, 10^2, 10^4, 10^6, and 10^8 have been solved by the computer. As Q^* increases, the starting step-size must decrease. For example, for $Q^* = 10^{-3}$, $h = 0.01$; $Q^* = 10^2$, $h = 0.001$; $Q^* = 10^8$, $h = 0.00001$. Otherwise the machine will print out "RESULT OUT OF RANGE IN FLFX." This means the magnitude of such a floating-point number exceeds the largest permissible number, $0.99999999 \times 10^{49}$. Therefore, proper step-size plays an important role in obtaining the required accuracy.

From Table 3 to Table 11 it can be noted that δ^* increases as x^* increases, and δ^* increases more rapidly than x^* does when values of x^* are small or $Q^* = 10^{-3}$. These observations are physically reasonable.

By substituting the values of x^* and δ^* into Equation (2-11), the non-dimensional surface velocity of liquid film in the x-direction can easily be obtained.

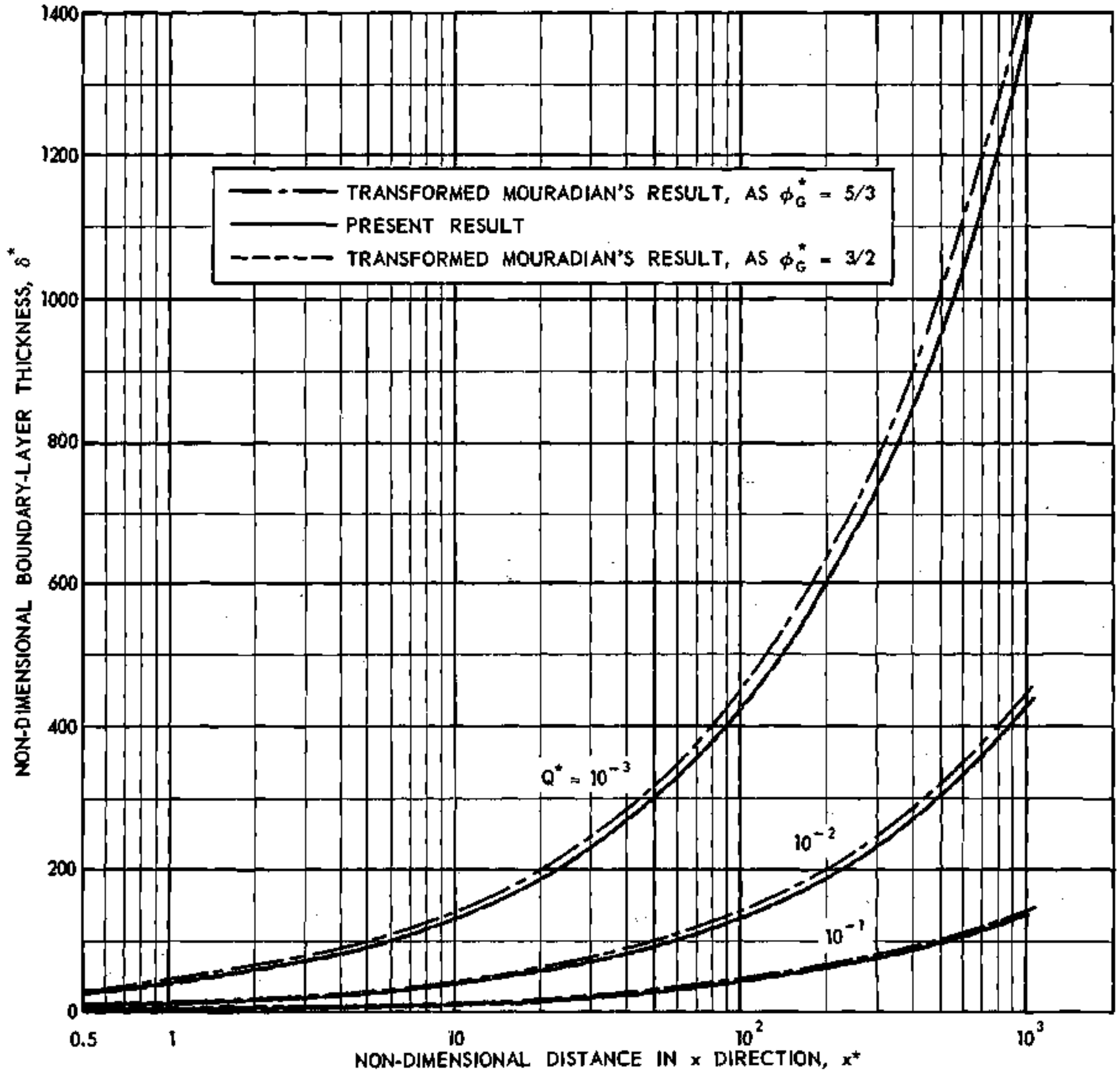

Figure 2. Boundary Layer Thickness of a Liquid Film Appearing on a Porous Wall or on a Solid-liquid Interface as Calculated by the Runge-Kutta Fourth-order Method with Burroughs 220 Computer and as Approximated by Transformed Mouradian's Results.

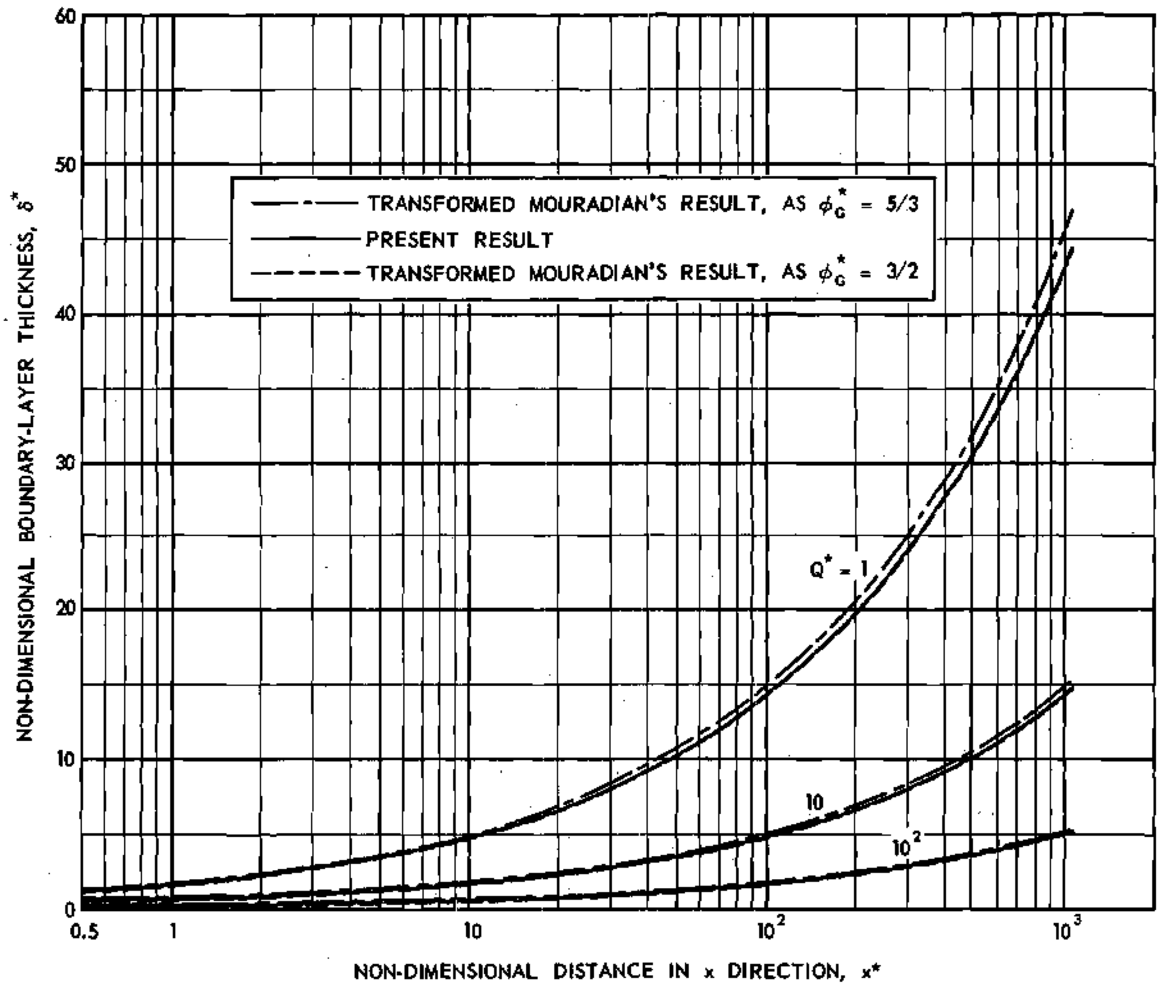

Figure 3. Boundary Layer Thickness of a Liquid Film Appearing on a Porous Wall or on a Solid-liquid Interface as Calculated by the Runge-Kutta Fourth-order Method with Burroughs 220 Computer and as Approximated by Transformed Mouradian's Results.

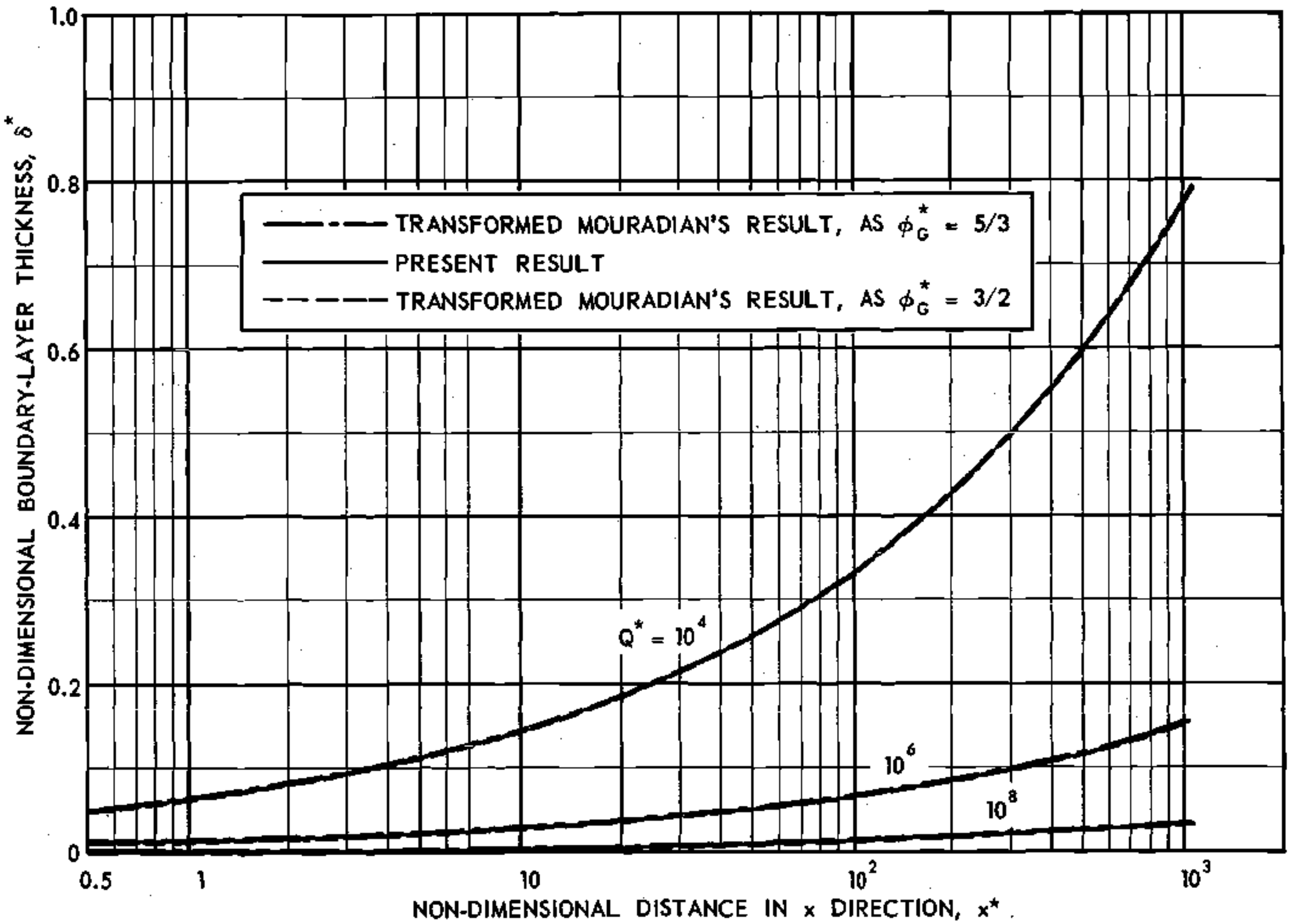

Figure 4. Boundary Layer Thickness of a Liquid Film Appearing on a Porous Wall or on a Solid-liquid Interface as Calculated by the Runge-Kutta Fourth-order Method with Burroughs 220 Computer and as Approximated by Transformed Mouradian's Results.

CHAPTER V

CONCLUSIONS

The purpose of this study was to investigate the laminar hydrodynamic boundary layer thickness and the velocity distribution within a liquid film appearing on a plane surface due to transpiration through a porous wall or the melting of a solid material.

The previous study that is most closely related to this one is that of Mouradian (20). The main differences between this study and the work of Mouradian are the form of the non-linear first-order differential equation for the hydrodynamic boundary layer thickness and the use of a different method of obtaining approximate solutions.

The calculations of this work were carried out by using Merson's modification of the Runge-Kutta fourth-order method with the Burroughs 220 Computer. The computer was operated in conformity with a program which was based on Equation (2-14b) and on the assumed starting point ($x^* = 0.0702$, $\delta^* = 0$) as well as on the different values of the non-dimensional parameter Q^*. The program used in this study is written according to the machine language of the Burroughs Algebraic Compiler — 220.

The proper step-size plays an important role in obtaining the required accuracy. For small enough variations in the initial conditions, the absolute value of the truncation error decreases as x^* increases. Therefore, it can be concluded that the Runge-Kutta fourth-order method of Merson for the given non-linear first-order differential is stable.

This numerical method gives good results. The lower limit expression for the film thickness

$$x^* = \frac{Q^* \quad \delta^{*3}}{1.8\ \delta^* + 3}$$

may be used as the approximate solution of Equation (2-14b) without serious error.

Tables listed in Appendix VII allow good application in the engineering field. From these tables, it can be seen that δ^* increases as x^* increases and δ^* increases more rapidly than x^* does when values of x^* are small or $Q^* = 10^{-3}$. These observations are physically reasonable.

The non-dimensional surface velocity of the liquid film in the x-direction is expressed as

$$U^* = 1.5\ \frac{x^*}{\delta^*}$$

Numerical values of this non-dimensional surface velocity of liquid film in the x-direction can easily be obtained by substituting the values of x^* and δ^* into the above equation. Then the velocity distribution of a certain point in the fluid can be determined by the following equation:

$$\frac{u^*}{U^*} = 2\eta - \eta^2$$

where

$$\eta = \frac{y}{\delta} \text{ or } \frac{y^*}{\delta^*}$$

APPENDICES

APPENDIX I

NOMENCLATURE

Symbol	
a	Coefficient in velocity profile polynomial
A	Coefficient in velocity profile polynomial
b	Coefficient in velocity profile polynomial
B	Coefficient in velocity profile polynomial
c	Coefficient in velocity profile polynomial
C	Coefficient in velocity profile polynomial
d	Coefficient in velocity profile polynomial
$f(\eta)$	Velocity profile function
F_x	External force in the x-direction lb_f
g	Gravitational acceleration in the x-direction, ft sec^{-2}
G	Gravitational acceleration, ft sec^{-2}
h	Step-size, or interval
H	Step-size in the computer program
k	Operation quantity of Runge-Kutta Method
L	Characteristic length; defined as $L = \frac{\nu}{V_o}$, ft
M_x	x momentum, lb_m ft sec^{-1}
Q^*	Non-dimensional quantity; defined as $Q^* = \frac{g\nu}{V_o^3} = \frac{gL}{V_o^2}$
Re_x	Local Reynolds number in the x-direction based on "feed in" velocity: $Re_x = \frac{V_o x}{\nu}$

Symbol

Re_δ	Local Reynolds number based on film thickness and "feed in" velocity; $Re = \frac{V_o \delta}{\nu}$
t	Temperature F^o
u	Velocity in x-direction within liquid film, ft sec^{-1}
u^*	Non-dimensional velocity in x-direction within liquid film; defined as $\frac{u}{V_o}$
U	Surface velocity of liquid film in x-direction, ft sec^{-1}
U^*	Non-dimensional surface velocity of liquid film in x-direction; defined as $\frac{U}{V_o}$
v	Velocity in y-direction within liquid film, ft sec^{-1}
V_o	"Feed in" velocity in the y-direction at the plane, ft sec^{-1}
x	Space coordinate parallel to plate, ft
x^*	Non-dimensional space coordinate parallel to plate, $\frac{x}{L}$
y	Space coordinate normal to plate, ft
y^*	Non-dimensional space coordinate normal to plate, $\frac{y}{L}$
z	Space coordinate normal to paper, ft

Greek Letters

α_1	Quantity defined as $\alpha = \int_o^1 f(\eta)\,d\eta$
α_2	Quantity defined as $\alpha = \int_o^1 f^2(\eta)\,d\eta$
β_1	Quantity defined as $\beta_1 = f'(0)$
δ	Liquid film thickness normal to the surface of the wall, ft

Greek Letters

δ^*	Non-dimensional liquid film thickness normal to the surface of the wall, $\frac{\delta}{L}$
Δ	Difference between values
ϵ	Truncation error
η	Dimensionless distance from wall; $\eta = \frac{y}{\delta}$ or $\frac{y^*}{\delta^*}$
ν	Kinematic viscosity; $ft^2\ sec^{-1}$
ρ	Density of Liquid, $lb_m\ ft^{-3}$
Σ	Summation
T	Time, sec
τ	Shearing stress, lb_f/ft^2
ϕ_G	Quantity appearing in Mouradian's work; defined as $\phi_G = \dfrac{\frac{3}{2}\frac{V_o}{\nu}\delta + \frac{25}{6}}{\frac{V_o}{\nu}\delta + \frac{5}{2}}$

Subscripts

crit	Critical value
δ	At $y = \delta$
max	Maximum
min	Minimum
w	At the wall

Superscript

*	Denotes dimensionless quantity

APPENDIX II

NON-DIMENSIONAL TRANSFORMATION

In this thesis, some equations can be simplified by non-dimensional transformations. For this purpose, some non-dimensional quantities are introduced:

$$x^* = \frac{x}{L} \qquad y^* = \frac{y}{L} \qquad \delta^* = \frac{\delta}{L} \tag{AII-1}$$

$$u^* = \frac{u}{V_o} \qquad U^* = \frac{U}{V_o} \tag{AII-2}$$

Where L, the characteristic length, is defined as:

$$L = \frac{\nu}{V_o} \tag{AII-3}$$

Then

$$Re_x = \frac{V_o x}{\nu} = \frac{x}{L} = x^* \tag{AII-4}$$

$$Re_\delta = \frac{V_o\,\delta}{\nu} = \frac{\delta}{L} = \delta^* \tag{AII-5}$$

In order to obtain Equation (2-14a) or Equation (2-14b), every term in Equation (2-13) must be non-dimensionalized.

$$\frac{d\delta}{dx} = \frac{d\delta}{d\delta^*}\frac{d\delta^*}{dx^*}\frac{dx^*}{dx} = L\,\frac{d\delta^*}{dx^*}\,\frac{1}{L} = \frac{d\delta^*}{dx^*}$$

$$\frac{\nu}{V_o}\,\frac{1}{x} = L\,\frac{1}{Lx^*} = \frac{1}{x^*}$$

$$\frac{\delta}{x} = \frac{L\delta^*}{Lx^*} = \frac{\delta^*}{x^*}$$

$$\frac{g}{V_o^{\,2}}\,\frac{\delta^3}{x^2} = \frac{g}{V_o^{\,2}}\,\frac{L^3\delta^{*3}}{L^2x^{*2}} = \frac{gL}{V_o^{\,2}}\,\frac{\delta^{*3}}{x^3} = \frac{g\,\nu}{V_o^{\,3}}\,\frac{\delta^{*3}}{x^{*2}} =$$

$$Q^*\,\frac{\delta^{*3}}{x^{*2}}$$

where

$$Q^* = \frac{g\,\nu}{V_o^{\,3}} = \frac{gL}{V_o^{\,2}} = \frac{gL^2}{V_o\,\nu} \qquad \text{(AII-6)}$$

Hence, the non-dimensional differential equation for the boundary layer thickness is:

$$\frac{d\delta^*}{dx^*} = \frac{5}{2}\,\frac{1}{x^*} + 2\,\frac{\delta^*}{x^*} - \frac{5}{6}\,Q^*\,\frac{\delta^{*3}}{x^{*2}} \qquad \text{(2-14a)}$$

or

$$\frac{d\delta^*}{dx^*} = \left(\frac{5}{2} + 2\delta^* - \frac{5}{6}\,Q^*\,\frac{\delta^{*3}}{x^*}\right)\frac{1}{x^*} \qquad \text{(2-14b)}$$

In Equation (AIII-2g), $\frac{g\delta^2}{\nu U}$ can be transformed as:

$$\frac{g\,\delta^2}{\nu U} = \frac{g\,\nu}{V_o^{\,3}}\,\frac{V_o^{\,2}\delta^2}{\nu^{\,2}}\,\frac{V_o}{U} = \frac{Q^*Re_\delta^{\,2}}{U^*} = \frac{Q^*\delta^{*2}}{U^*}$$

APPENDIX III

VELOCITY DISTRIBUTION WITH FOUR BOUNDARY CONDITIONS

Mouradian (20) used the four boundary conditions, Equations (2-3a) through (2-3d) to get a polynomial of the fourth degree for the velocity function in terms of the dimensionless distance from the wall.

If the four boundary conditions are used, the velocity profile can be assumed to be:

$$\frac{u\ (x,y)}{U\ (x)} = f\ \left(\frac{y}{\delta (x)} \right) = f(\eta) = a + b\eta + c\eta^2 + d\eta^3 \qquad \text{(AIII-1)}$$

Equation (2-3a) gives:

$$a = 0 \qquad \text{(AIII-2a)}$$

From Equation (2-3b), that is, at $\eta = 1$, $f(\eta) = 1$,

$$b + c + d = 1 \qquad \text{(AIII-2b)}$$

The first derivative of Equation (AIII-1) with respect to y is:

$$\frac{\partial u}{\partial y} = U\ \left[\frac{b}{\delta} + \frac{2c}{\delta} \left(\frac{y}{\delta} \right) + \frac{3d}{\delta} \left(\frac{y}{\delta} \right)^2 \right]$$

At $y = \delta$

$$\left(\frac{\partial u}{\partial y} \right)_{y=\delta} = \frac{U}{\delta}\ (b + 2c + 3d)$$

Then, Equation (2-3c) gives:

$$b + 2c + 3d = 0 \tag{AIII-2c}$$

At y = 0, the first derivative of u with respect to y becomes:

$$\left(\frac{\partial u}{\partial y}\right)_{y=o} = \frac{Ub}{\delta}$$

The second derivative of Equation (AIII-1) with respect to y is:

$$\frac{\partial^2 u}{\partial y^2} = U \left[\frac{2c}{\delta^2} \quad \frac{6d}{\delta^2} \left(\frac{y}{\delta}\right) \right]$$

At y = 0

$$\left(\frac{\partial^2 u}{\partial y^2}\right)_{y=o} = \frac{2Uc}{\delta^2}$$

Then, Equation (2-3d) gives:

$$\frac{V_o U}{\delta} b = g + \frac{2\ U}{\delta^2} c \tag{AIII-2d}$$

From Equations (AIII-2b) and (AIII-2c)

$$2b + c = 3$$

$$c = 3 - 2b \tag{AIII-2e}$$

Substituting Equation (AIII-2e) into Equation (AIII-2b) gives:

$$d = 1 - b - 3 + 2b$$

$$d = b - 2 \tag{AIII-2f}$$

Substituting Equation (AIII-2e) into Equation (AIII-2d) gives:

$$\left(\frac{V_o\delta}{\nu} + 4\right) b - 6 = \frac{g\delta^2}{\nu U}$$

or

$$b = \frac{\dfrac{g\delta^2}{\nu U} + 6}{\dfrac{V_o\delta}{\nu} + 4} \qquad \text{(AIII-2g)}$$

From Appendix II, Equation (AIII-2g) can be rewritten in a non-dimensional form:

$$b = \frac{\dfrac{Q^* Re_\delta^{\ 2}}{U^*} + 6}{Re_\delta + 4} \qquad \text{(AIII-2h)}$$

or

$$b = \frac{\dfrac{Q^* \delta^{*2}}{U^*} + 6}{\delta^* + 4} \qquad \text{(AIII-2i)}$$

Substituting Equations (AIII-2a), (AIII-2e), and (AIII-2f) into Equation (AIII-1) gives:

$$\frac{u}{U} = b\,\eta + (3 - 2b)\eta^2 + (b-2)\,\eta^3$$

$$\frac{u}{U} = b\ (\eta - 2\,\eta^2 + \eta^3) + (3\eta^2 + 2\,\eta^3) \qquad \text{(AIII-3)}$$

or

$$\frac{u^*}{U^*} = b\ (\eta - 2\eta^2 + \eta^3) + (3\eta^2 + 2\,\eta^3) \qquad \text{(AIII-4)}$$

As stated by Mouradian, "The terms δ and U remain to be obtained from the solution of the continuity and momentum equations. Then, b_G (i.e. b in this thesis) can be determined explicitly." (20).

APPENDIX IV

THE DETERMINATION OF THE RANGES OF Q*

Before Equation (2-14b) can be solved by a numerical method with the electronic computer, the range of Q* must be determined. In Appendix II, Q* is defined as:

$$Q^* = \frac{g\,\nu}{V_o^3} \quad \frac{gL}{V_o^2} = \frac{gL^2}{V_o\,\nu}$$

The above expression implies that the ranges of Q* are determined by the ranges of g, ν, and V_o. This will be discussed respectively, as follows:

1. As assumed in Chapter II, the fluid flows along the surface of the wall under the influence of gravity. Therefore, the case of the horizontal plane is not included in this thesis and the ranges of g, the gravitational acceleration in the x-direction, are selected from 8.34 ft/sec^2 (i.e., 32.2 COS 75^o) to 32.2 ft/sec^2 (i.e., 32.2 COS 0^o).

2. From Table 1 (listed at end of Appendix IV, Page 42) which is taken from References (17), (26) and (27), the ranges of ν, kinematic viscosity, are selected from 0.07 x 10^{-5} ft^2/sec to 2 x 10^{-2} ft^2/sec.

3. In order to define the ranges of V_o, the following assumptions are made:

(a) A critical Reynolds number of 1080[1] in the x-direction is assumed. According to Appendix II, then $(x^*)_{crit} = (Re_x)_{crit} = 1080$.

(b) A minimum critical point at x = 0.5 in and a maximum critical point at x = 20 ft.

If $(x_{crit})_{min} = 0.5$ in $= 0.0417$ ft, then

$$V_o = (V_o)_{max} = \frac{1080 \times (\nu)_{max}}{(x_{crit})_{min}} = \frac{1080 \times 2 \times 10^{-5}}{0.0417} = 0.518 \text{ ft/sec}$$

$$L = \frac{\nu}{V_o} = \frac{2 \times 10^{-5}}{0.518} = 3.86 \times 10^{-5}$$

$$Q^* = \frac{gL}{V_o^2} \quad \frac{g\,\nu}{V_o^3}$$

$$Q^* = \frac{(g)_{min}\,L}{V_o^2} \quad \frac{(g)_{min}\,\nu}{V_o^3} \quad \frac{8.34 \times 2 \times 10^{-5}}{0.518^3}$$

$$= 1.196 \times 10^{-3}$$

If $(x_{crit})_{max} = 20$ ft

---

[1]Duker and Bergelin (28) experimentally investigated the characteristics of water film flowing down a vertical surface. They found that transition from laminar to turbulent film flow occurs at a Reynolds number of 1080 when the Reynolds number is based on the average velocity in the film and film thickness.

$$Re = \frac{\bar{u}}{\nu} = \frac{\left[\frac{1}{\delta}\int_0^{\delta} u\,dy\right]\delta}{\nu} = \frac{\left[\frac{1}{\delta}\ \frac{2}{3}\,U\,\delta\ \right]\ \delta}{\nu} = \frac{\frac{2}{3}\,U\,\delta}{\nu} = \frac{V_o x}{\nu} = Re_x$$

$$= \frac{x}{L} = x^*$$

$$V_o = (V_o)_{min} = \frac{1080 \times (\nu)\ min}{(x_{crit})_{max}} \quad \frac{1080 \times 0.07 \times 10^{-5}}{20}$$

$$= 3.78 \times 10^{-5} \text{ ft/sec}$$

$$L = \frac{\nu}{V_o} = \frac{0.07 \times 10^{-5}}{3.78 \times 10^{-5}} = 1.853 \times 10^{-2}$$

$$Q^* = \frac{gL}{V_o^2} = \frac{g\nu}{V_o^3}$$

$$Q^* = \frac{(g)_{max} L}{V_o} = \frac{(g)_{max}\ \nu}{V_o^3} = \frac{32.2 \times 0.07 \times 10^{-5}}{(3.78 \times 10^{-5})^3} = 4.47 \times 10^8$$

From the above calculations, the ranges of Q* are selected from 1.196×10^{-3} to 4.47×10^8. However, for the computer calculation, the ranges of Q* are selected from 10^{-3} to 10^8.

Table 1[1]. Property Values

Substance	Range of t, F	Range of ν, $ft.^2/sec.$	Substance	Range of t, F	Range of ν, $ft.^2/sec.$
Fluid in Saturated State			**Liquid Metals**		
Ammonia	-58 122	0.355×10^{-5} 0.468	Bismuth	600 1400	0.090×10^{-5} 0.174
Carbon dioxide	-58 86	0.086 0.128	Lead	700 1300	0.145 0.245
Freon 12	-58 122	0.204 0.334	Mercury	32 600	0.072 0.133
Methylchloride	-58 122	0.295 0.344	Na,56wt% K,44wt%	200 1300	0.234 0.702
Sulfur dioxide	-58 122	0.174 0.521	Na,22wt% K,78wt%	200 1400	0.228 0.624
Water	32 600	0.137 1.930	Pb,44.5wt% Bi,55.5wt%	300 1200	0.161 0.126

[1]This table is taken from References (17), (26), and (27).

APPENDIX V

DISCUSSION OF THE POINT AT $x^* = 0$, $\delta^* = 0$

It is known that Equation (2-14b) has a singular point at $x^* = 0$, $\delta^* = 0$ (i.e., $x = 0$, $\delta = 0$). This fact causes difficulty in the computer calculation. Therefore, to make an assumption that the initial condition is $x = 1.3 \times 10^{-3}$ ft (or $\frac{1}{64}$ in), $\delta = 0$ instead of the given boundary condition $x = 0$, $\delta = 0$ is necessary.

Now these two values will be transformed into non-dimensional values. In the case of

$$L = 1.853 \times 10^{-2}$$

$$x^* = \frac{x}{L} = \frac{1.3 \times 10^{-3}}{1.853 \times 10^{-3}} = 0.702 \times 10^{-1} = 0.0702$$

$$\delta^* = \frac{\delta}{L} = 0$$

For $L = 3.86 \times 10^{-5}$,

$$x^* = \frac{x}{L} \frac{1.3 \times 10^{-3}}{3.86 \times 10^{-5}} = 0.337 \times 10^{2} = 33.7$$

$$\delta^* = \frac{\delta}{L} = 0$$

Then, an assumed point at $x^* = 0.0702$, $\delta^* = 0$ will be used as the initial condition for calculation. As discussed in Chapter IV, this assumption does not affect the desired numerical solution significantly.

APPENDIX VI

COMPUTER PROGRAM

An example of the program which is actually used in this study and is written according to the machine language of the Burroughs Algebraic Compiler (29), is given below. In this program, Y stands for δ^*, Q for Q^*, X for x^*, H for the step-size h.

```
2COMMENT A CALCULATION FOR HYDRODYNAMIC BOUNDARY LAYER THICKNESS
         BY C. S. LU                                                  $
2        INTEGER I                                                    $
2ARRAY   XS(3)=(0.0702,1.0802,11.5802)                                $
2ARRAY   HS(3)=(0.001,0.01,0.5)                                       $
2ARRAY   XF(3)=(1.0702,11.0802,1080.5802)                             $
2        Y=0.0  $  Q=1.0**2                                           $
2        WRITE ($$DOG1,CAT1)                                          $
2        WRITE ($$TITLE)                                              $
2        FOR I=(1,1,3)                                                $
2        FOR X=(XS(I),HS(I),XF(I))                                    $
2BEGIN   H=HS(I)                                                      $
2        K1=H.(2.Y+2.5-(0.833.Q.Y*3)/X)/(3.X)                         $
2        K2=H.(2.(Y+K1)+2.5-(0.833.Q.(Y+K1)*3)/(X+(H/3)))/(3.X+H)     $
2        K3=H.(2.(Y+0.5.K1+0.5.K2)+2.5-(0.833.Q.(Y+0.5.K1+
         0.5.K2)*3)/(X+(H/3)))/(3.X+H)                                $
2        K4=H.(2.(Y+0.375.K1+1.125.K3)+2.5-(0.833.Q.(Y+0.375.K1+
         1.125.K3)*3)/(X+0.5.H)))/(3.X+(1.5.H))                       $
```

```
2        K5=H.(2.(Y+1.5.K1-4.5.K3+6.K4)+2.5-(0.833.Q.(Y+1.5.K1-
            4.5.K3+6.K4)*3)/(X+H))/(3.(X+H))                          $
2        YH=Y+0.5(K1+4.K4+K5)                                          $
2        WRITE ($$DOG2,CAT2)  $  Y=YH  END                             $
2OUTPUT  ((DOG1(Y,Q)),(DOG2(X,Y,K1,K2,K3,K4,K5)))                      $
2FORMAT  CAT1(B8,*Y=*,X10.8,B8,*Q=*,F12.6,W2)                          $
2FORMAT  TITLE  (B5,*X*,B14,*Y*,B16,*K1*,B16,*K2*,B16,*K3*,B16,
                *X4*,B16,*K5*,W2)                                      $
2FORMAT  CAT2(X10.5,B6,X10.8,B4,5F16.6,W0)                             $
2        FINISH                                                        $
```

APPENDIX VII

DATA

The numerical solution of Equation (2-14b) is carried out by the Runge-Kutta fourth-order method of Merson (21) with the Burroughs 220 Computer. The computer results are obtained in the form of a typewritten numerical table which directly gives X (standing for x^*), Y (representing δ^*), K1, K2, K3, K4 and K5, as shown in Table 2. The cases for $Q^* = 10^{-3}$, 10^{-2}, 0.1, 1.0, 10, 10^2, 10^4, 10^6, and 10^8 have been solved by the computer and the results are listed in Tables 3 to 11.

Table 2. Numerical Results — Reproduction of Computer Print-out

Y = .000000 Q = .100000,-2

X	Y	K1	K2	K3	K4	K5
.0702	.00000	.118708, 00	.124088, 00	.124332, 00	.127159, 00	.135597, 00
.0802	.38147	.135592, 00	.140971, 00	.141185, 00	.143986, 00	.152324, 00
.0902	.81340	.152322, 00	.157641, 00	.157828, 00	.160577, 00	.168735, 00
.1002	1.29508	.168732, 00	.173934, 00	.174097, 00	.176765, 00	.184655, 00
.1102	1.82530	.184653, 00	.189675, 00	.189816, 00	.192374, 00	.199906, 00
.1202	2.40233	.199905, 00	.204686, 00	.204806, 00	.207224, 00	.214309, 00
.1302	3.02389	.214308, 00	.218786, 00	.218887, 00	.221135, 00	.227687, 00
.1402	3.68716	.227686, 00	.231804, 00	.231887, 00	.233939, 00	.239876, 00
.1502	4.38882	.239875, 00	.243581, 00	.243647, 00	.245478, 00	.250732, 00
.1602	5.12508	.250732, 00	.253980, 00	.254031, 00	.255621, 00	.268000, 00
.1702	5.89176	.260136, 00	.262892, 00	.262931, 00	.264264, 00	.264273, 00
.1802	6.68436	.268000, 00	.270241, 00	.270269, 00	.271337, 00	.274273, 00
.1902	7.49817	.274273, 00	.275988, 00	.276006, 00	.276807, 00	.278940, 00
.2002	8.32839	.278940, 00	.280131, 00	.280142, 00	.280677, 00	.282024, 00
.2102	9.17023	.282024, 00	.282704, 00	.282709, 00	.282989, 00	.283582, 00
.2202	10.01901	.283582, 00	.283776, 00	.283777, 00	.283816, 00	.283704, 00
.2302	10.87029	.283704, 00	.283445, 00	.283444, 00	.283260, 00	.282502, 00
.2402	11.71991	.282502, 00	.281832, 00	.281830, 00	.281446, 00	.280109, 00
.2502	12.56411	.280109, 00	.279075, 00	.279072, 00	.278512, 00	.276671, 00

X - represents x^*

Y - represents δ^*

K1 - represents $K_1 = \frac{1}{3} hf\,(x_n^*, \delta_n^*)$, where h is the step-size

K2 - represents $K_2 = \frac{1}{3} hf\,(x_n^* + \frac{1}{3} h, \delta_n^* + K_1$

K3 - represents $K_3 = \frac{1}{3} hf\,(x_n^* + \frac{1}{3} h, \delta_n^* + \frac{1}{2} K_1 + \frac{1}{2} K_2)$

K4 - represents $K_4 = \frac{1}{3} hf\,(x_n^* + \frac{1}{2} h, \delta_n^* + \frac{3}{8} K_1 + \frac{9}{8} K_3)$

K5 - represents $K_5 = \frac{1}{3} hf\,(x_n^* + h, \delta_n^* + \frac{3}{2} K_1 - \frac{9}{2} K_3 + 6K_4)$

Table 3. Tabulation of x* Versus δ* with Q* = 10^{-3}

x*	δ*	x*	δ*
0.5002	28.21222	220.0702	630.50746
1.0002	42.93019	240.0702	658.49060
5.0002	95.85940	260.0702	685.33046
10.0202	135.64369	280.0702	711.15665
15.0702	165.72003	300.0702	736.07602
20.0702	191.09559	340.0702	783.53779
25.0702	213.46163	380.0702	828.28103
30.0702	233.68766	420.0702	870.72543
35.0702	252.29096	460.0702	911.19274
40.0702	269.60889	500.0702	949.93590
45.0702	285.87599	540.0702	987.15810
50.0702	301.26308	580.0702	1023.02290
60.0702	329.88463	620.0702	1057.67070
70.0702	356.20735	660.0702	1091.21830
80.0702	380.70966	700.0702	1123.76440
90.0702	403.72396	740.0702	1155.39280
100.0702	425.49236	780.0702	1186.17770
120.0702	465.98181	820.0702	1216.18280
140.0702	503.21750	860.0702	1245.46490
160.0702	537.87682	900.0702	1274.07250
180.0702	570.43047	1000.0702	1342.92910
200.0702	601.22109	1079.5702	1395.24530

Table 4. Tabulation of x* Versus δ* with $Q^* = 10^{-2}$

x*	δ*	x*	δ*
0.5002	10.27813	220.0702	200.05746
1.0002	14.29060	240.0702	208.90687
5.0002	30.94228	260.0702	217.39473
10.0202	43.43046	280.0702	225.56197
15.0702	53.05411	300.0702	233.44240
20.0702	61.08280	340.0702	248.45154
25.0702	68.15853	380.0702	262.60096
30.0702	74.55680	420.0702	276.02340
35.0702	80.44144	460.0702	288.82057
40.0702	85.91929	500.0702	301.07242
45.0702	91.06460	540.0702	312.84325
50.0702	95.93144	580.0702	324.18565
60.0702	104.98398	620.0702	335.14326
70.0702	113.30922	660.0702	345.75275
80.0702	121.05856	700.0702	356.04537
90.0702	128.33717	740.0702	366.04788
100.0702	135.22165	780.0702	375.78362
120.0702	148.02671	820.0702	385.27270
140.0702	159.80256	860.0702	394.53303
160.0702	170.76354	900.0702	403.58041
180.0702	181.05850	1000.0702	425.35577
200.0702	190.79585	1079.5702	441.90052

Table 5. Tabulation of x* Versus δ* with Q* = 0.1

x*	δ*	x*	δ*
0.5002	3.67483	220.0702	63.91811
1.0002	4.97384	240.0702	66.71772
5.0002	10.32835	260.0702	69.40286
10.0202	14.30853	280.0702	71.98650
15.0702	17.36757	300.0702	74.47936
20.0702	19.91646	340.0702	79.22714
25.0702	22.16117	380.0702	83.70282
30.0702	24.18996	420.0702	87.94843
35.0702	26.05523	460.0702	91.99617
40.0702	27.79107	500.0702	95.87138
35.0702	29.42123	540.0702	99.59440
50.0702	30.96288	580.0702	103.18151
60.0702	33.82986	620.0702	106.64695
70.0702	36.46597	660.0702	110.00229
80.0702	38.91933	700.0702	113.25740
90.0702	41.22340	740.0702	116.42076
100.0702	43.40249	780.0702	119.49970
120.0702	47.45512	820.0702	122.50067
140.0702	51.18159	860.0702	125.42928
160.0702	54.64990	900.0702	128.29063
180.0702	57.90725	1000.0702	135.17703
200.0702	60.98800	1079.5702	140.40924

Table 6. Tabulation of x^* Versus δ^* with $Q^* = 1.0$

x^*	δ^*	x^*	δ^*
0.5002	1.42132	220.0702	20.81606
1.0002	1.87507	240.0702	21.70415
5.0002	3.67440	260.0702	22.55575
10.0702	4.98882	280.0702	23.37501
15.0702	5.97025	300.0702	24.16536
20.0702	6.79311	340.0702	25.67032
25.0702	7.51553	380.0702	27.08870
30.0702	8.16703	420.0702	28.43393
35.0702	8.76503	460.5702	29.73193
40.0702	9.34083	500.0702	30.94377
45.0702	9.84224	540.0702	32.12294
50.0702	10.33491	580.0702	33.25907
60.0702	11.25018	620.0702	34.35654
70.0702	12.09083	660.0702	35.41906
80.0702	12.87253	700.0702	36.44970
90.0702	13.60617	740.0702	37.45133
100.0702	14.29962	780.0702	38.42613
120.0702	15.58844	820.0702	39.37619
140.0702	16.77272	860.0702	40.30329
160.0702	17.87436	900.0702	41.20904
180.0702	18.90856	1000.0702	43.38883
200.0702	19.88635	1079.5702	45.04489

Table 7. Tabulation of x* Versus δ* with Q* = 10

x*	δ*	x*	δ*
0.5002	0.5927300	220.0702	7.0828681
1.0002	0.7661700	240.0702	7.3686080
5.0702	1.4289499	260.0702	7.6423542
10.0702	1.8802462	280.0702	7.9054912
15.0702	2.2167479	300.0702	8.1591579
20.0702	2.4958580	340.0702	8.6417250
25.0702	2.7390823	380.0702	9.0960424
30.0702	2.9572114	420.0702	9.5265357
35.0702	3.1565520	460.0702	9.9365864
40.0702	3.3411613	500.0702	10.3288160
45.0702	3.5138277	540.0702	10.7053830
50.0702	3.6765637	580.0702	11.0680260
60.0702	3.9779312	620.0702	11.4181650
70.0702	4.2537638	660.0702	11.7570140
80.0702	4.5095387	700.0702	12.0855950
90.0702	4.7490275	740.0702	12.4047870
100.0702	4.9749558	780.0702	12.7153490
120.0702	5.3938433	820.0702	13.0179430
140.0702	5.7777454	860.0702	13.3131530
160.0702	6.1341180	900.0702	13.6014920
180.0702	6.4681024	1000.0702	14.2951590
200.0702	6.7834206	1079.5702	14.8219290

Table 8. Tabulation of x* Versus δ* with $Q^* = 10^2$

x*	δ*	x*	δ*
0.5002	0.26006027	220.0702	2.59359680
1.0002	0.33194891	240.0702	2.68973690
5.0002	0.59265318	260.0702	2.78162680
10.0002	0.76612200	280.0702	2.86977050
15.0702	0.89399291	300.0702	2.95457910
20.0702	0.99696949	340.0702	3.11550720
25.0702	1.08580060	380.0702	3.26656400
30.0702	1.16483110	420.0702	3.40933280
35.0702	1.23658040	460.0702	3.54501660
40.0702	1.30265800	500.0702	3.67455530
45.0702	1.36416360	540.0702	3.79869950
50.0702	1.42188720	580.0702	3.91805890
60.0702	1.52820660	620.0702	4.03313800
70.0702	1.62491850	660.0702	4.14435900
80.0702	1.61413500	700.0702	4.25207840
90.0702	1.79730140	740.0702	4.35660220
100.0702	1.87545640	780.0702	4.45819470
120.0702	2.01965400	820.0702	4.55708550
140.0702	2.15108090	860.0702	4.65347640
160.0702	2.27252650	900.0702	4.74754500
180.0702	2.38590190	1000.0702	4.97354930
200.0702	2.49258230	1079.5702	5.14491540

Table 9. Tabulation of x* Versus δ* with Q* = 10^4

x*	δ*	x*	δ*
0.57214	0.05437114	220.28314	0.44002143
1.07214	0.06944101	240.28314	0.45401282
5.07214	0.11765625	260.28314	0.46730235
10.07214	0.14875000	280.28314	0.47997641
15.00314	0.17114445	300.28314	0.49210539
20.00314	0.18902610	340.28314	0.51495183
25.08314	0.20444653	380.28314	0.53620592
30.08314	0.21777336	420.28314	0.55613355
35.08314	0.22974871	460.28314	0.57447786
40.08314	0.24067878	500.28314	0.59276761
45.08314	0.25077142	540.28314	0.60975353
50.08314	0.26017514	580.28314	0.62599327
60.08314	0.27733084	620.28314	0.64156904
70.08314	0.29276075	660.28314	0.65654929
80.08314	0.30685516	700.28314	0.67099177
90.08314	0.31987939	740.28314	0.68494568
100.08314	0.33202296	780.28314	0.69845328
120.08314	0.35419790	820.28314	0.71155125
140.28314	0.37431804	860.28314	0.72427159
160.28314	0.39259585	900.28314	0.73664243
180.28314	0.40947208	1000.28310	0.76619743
200.28314	0.42522034	1079.28310	0.78832051

Table 10. Tabulation of x^* Versus δ^* with $Q^* = 10^6$

x^*	δ^*	x^*	δ^*
0.51270	0.01448203	220.42370	0.08881395
1.21270	0.01526458	240.42370	0.09147333
5.21270	0.02514572	260.42370	0.09399169
10.21270	0.03150840	280.42370	0.09638657
15.00370	0.03585741	300.42370	0.09867229
20.00370	0.03949642	340.42370	0.10296150
25.02370	0.04258540	380.42370	0.10693331
30.02370	0.04527757	420.42370	0.11064122
35.02370	0.04768778	460.42370	0.11412581
40.02370	0.04988037	500.42370	0.11741843
45.02370	0.05189895	540.42370	0.12054392
50.02370	0.05377464	580.42370	0.12352234
60.02370	0.05718415	620.42370	0.12637014
70.02370	0.06023727	660.42370	0.12910103
80.02370	0.06301530	700.42370	0.13172650
90.02370	0.06557338	740.42370	0.13425640
100.02370	0.06795082	780.42370	0.13669911
120.02370	0.07227348	820.42370	0.13906191
140.42370	0.07621915	860.42370	0.14135117
160.42370	0.07973717	900.42370	0.14357251
180.42370	0.08297818	1000.42370	0.14885956
200.42370	0.08599156	1079.42370	0.15279915

Table 11. Tabulation of x^* Versus δ^* with $Q^* = 10^8$

x^*	δ^*	x^*	δ^*
0.50623	0.00247772	220.20623	0.01884433
1.00623	0.00311561	240.20623	0.01940075
5.00623	0.00532167	260.20623	0.01992720
10.00623	0.00669093	280.20623	0.02042744
15.00623	0.00767675	300.20623	0.02090451
20.00623	0.00845213	340.20623	0.02179879
25.00623	0.00910591	380.20623	0.02262576
30.00623	0.00967756	420.20623	0.02339685
35.00623	0.01018887	460.20623	0.02412067
40.00623	0.01065364	500.20623	0.02480388
45.00623	0.01108122	540.20623	0.02545176
50.00623	0.01147826	580.20623	0.02606857
60.00623	0.01219932	620.20623	0.02665779
70.00623	0.01284431	660.20623	0.02722234
80.00623	0.01343061	700.20623	0.02776464
90.00623	0.01397002	740.20623	0.02828679
100.00623	0.01447092	780.20623	0.02879057
120.00623	0.01538067	820.20623	0.02927751
140.20623	0.01621782	860.20623	0.02974896
160.20623	0.01694141	900.20623	0.03020610
180.20623	0.01762156	1000.20620	0.03129264
200.20623	0.01825326	1079.20620	0.03210167

BIBLIOGRAPHY

1. Adams, M. C., "Recent Advances in Ablation," American Rocket Society Journal, Vol. 29, No. 9, pp. 625-632 (September, 1959).

2. Bethe, H. A. and M. C. Adams, "A Theory for Ablation of Glassy Materials," Journal of the Aero/Space Science, Vol. 26, No. 6, pp. 321-328 (June, 1959).

3. Roberts, L.,"On the Melting of a Semi-Infinite Body of Ice Placed in a Hot Stream of Air," Journal of Fluid Mechanics, Vol. 4, pp. 505-528 (1958).

4. Lees, L., "Similarity Parameters for Surface Melting of a Blunt Nosed Body in a High Velocity Gas Stream," American Rocket Society Journal, Vol. 29, No. 5, pp. 345-354 (May, 1959).

5. Sutton, G. W., "The Hydrodynamics and Heat Conduction of a Melting Surface," Journal of the Aeronautical Sciences, Vol. 25, No. 1, pp. 29-32 (January, 1958).

6. Turcotte, D. L., "The Melting of Ice in a Hot Humid Stream of Air," Journal of Fluid Mechanics, Vol. 8, pp. 123-129 (May, 1960).

7. Citron, S. J., "Steady-State Melting of a Semi-Infinite Medium with Temperature-Dependent Properties," Journal of the Aero/Space Science, Vol. 27, No. 6, pp. 470-472 (June, 1960).

8. Duwez, P. and H. L. Wheeler, Jr., "Experimental Study of Cooling by Injection of a Fluid through a Porous Material," Journal of the Aeronautical Sciences, Vol. 15, No. 9, pp. 509-552 (September, 1948).

9. Wheeler, H. L., Jr. and P. Duwez, "Heat Transfer through Sweat-cooled Porous Tubes," Jet Propulsion, Vol. 25, pp. 519-524 (October, 1955).

10. Berman, A. S., "Laminar Flow in Channels with Porous Walls," Journal of Applied Physics, Vol. 24, pp. 1232-1235 (1953).

11. Yuan, S. W., "Further Investigation of Laminar Flow in Channels with Porous Walls," Journal of Applied Physics, Vol. 27, pp. 267-269 (1956).

12. Eckert, E. R. G. and J. N. B. Livingood, "Comparison of Effectiveness of Convection-, Transpiration-, and Film-Cooling Methods with Air as Coolant," N.A.C.A. Technical Report 1182, pp. 593-609 (1954).

13. Yuan, S. W. and A. B. Finkelstein, "Laminar Pipe Flow with Injection and Suction through a Porous Wall," Transactions of American Society of Mechanical Engineering, Vol. 78, pp. 719-724 (1956).

14. Hartnett, J. P. and E. R. G. Eckert, "Mass-transfer Cooling in a Laminar Boundary Layer with Constant Fluid Properties," Transactions of American Society of Mechanical Engineering, Vol. 79, pp. 247-254 (1957).

15. Eckert, E. R. G., P. J. Schneider, A. A. Hayday, and R. M. Larson, "Mass-transfer Cooling of a Laminar Boundary Layer by Injection of a Light-weight Foreign Gas," Jet Propulsion, Vol. 28, pp. 34-39 (January, 1958).

16. Leadon, B. M., "Some Experimental Techniques in Mass Transfer Cooling," Aero/Space Engineering, Vol. 18, pp. 28-32 (October, 1959).

17. Eckert, E. R. G. and R. M. Drake, Jr., Heat and Mass Transfer, McGraw-Hill Co., New York, pp. 301-315; 500-510 (1959).

18. Beusman, C. C. and J. Weisman, "Comparison of Transpiration and Ablation Cooling," American Rocket Society Journal, Vol. 30, pp. 573-574 (June, 1960).

19. Eichhorn, R., "The Effect of Mass Transfer on Free Convection," Transactions of American Society of Mechanical Engineering, Journal of Heat Transfer, pp. 260-263 (August, 1960).

20. Mouradian, E. M., Velocity and Temperature Distributions in a Liquid Film, Ph.D. Thesis, Northwestern University, Evanston, Illinois (September, 1961).

21. Lance, G. N., Numerical Methods for High Speed Computer, London Iliffe & Sons, Ltd. (1960).

22. Hamming, R. W., "Stable Predictor-corrector Method for Ordinary Differential Equations," Journal of the Association for Computing Machinery, Vol. 6, pp. 37-47 (1959).

23. Milne, W. E. and R. R. Reynolds, "Stability of a Numerical Solution of Differential Equations," Journal of the Association for Computing Machinery, Vol. 6, pp. 196-203 (1959).

24. Martin, D. W., "Runge-Kutta Methods for Integrating Differential Equations on High-speed Digital Computers," The Computer Journal, Vol. 1, pp. 118-123 (April, 1958 - January, 1959).

25. Carr, III, J. W., "Error Bounds for the Runge-Kutta Single-step Integration Process," Journal of the Association for Computing Machinery, Vol. 5, pp. 39-44 (March, 1958).

26. Kreith, F., Principles of Heat Transfer, International Textbook Company, Scranton, Pennsylvania, pp. 533-539 (1958).

27. Liquid-Metals Handbooks, 2nd ed., U. S. Government Printing Office,

Washington, D. C. (1952).

28. Dukler, A. E., and O. P. Bergelin, "Characteristics of Flow in Falling Liquid Films," Chemical Engineering Progress, Vol. 48, No. 2, pp. 557-563 (1952).

29. Burroughs Corporation, Burroughs Algebraic Compiler, Detroit (1961).